Inorg. Chem. **2008**, *47*, 2049−2055

Solvent-Assisted Spontaneous Resolution of a 16-Membered Ring Containing Gold(I) Showing Short Au···Au Aurophilic Interaction and a Figure-Eight Conformation

Tünde Tunyogi, Andrea Deák,* Gábor Tárkányi, Péter Király, and Gábor Pálinkás*

Institute of Structural Chemistry, Chemical Research Center, Hungarian Academy of Sciences, P.O. Box 17, H-1525, Budapest, Hungary

Received October 17, 2007

The achiral 4,6-bis(diphenylphosphino) phenoxazine (nixantphos) ligand was used to synthesize a gold(I) complex, $[Au_2(nixantphos)_2](NO_3)_2$, containing a 16-membered $[Au_2(nixantphos)_2]^{+2}$ cationic ring in a chiral figure-eight conformation. The single crystal X-ray diffraction analysis of $[Au_2(nixantphos)_2](NO_3)_2 \cdot 3MeOH \cdot H_2O$ (**1**) and $[Au_2(nixantphos)_2](NO_3)_2 \cdot 4MeCN$ (**2**) revealed a solvent-assisted spontaneous resolution of the $[Au_2(nixantphos)_2](NO_3)_2$ complex. By changing the nature of the solvent, homochiral hydrogen bonded helices (**1**) and heterochiral hydrogen bonded monomers (**2**) were obtained. Multinuclear NMR spectroscopy showed the evidence of chemical exchange phenomenon related to the interconversion of the enantiomeric skeletons of the 16-membered macrocycle in solution. The existence of the Au···Au aurophilic interaction was confirmed by the analysis of the spin-system in the ^{31}P NMR spectrum.

Introduction

The design and construction of chiral self-assembled supermolecules are among the most challenging tasks of supramolecular chemistry and crystal engineering, and the resulting chiral compounds also are of great current interest since their mechanical, optical, electric, magnetic properties make them promising candidates for advanced materials.[1] Chiral metal supermolecules are generally constructed by *stereoselective synthesis* using chiral species[2] or *spontaneous resolution*,[3] which does not require any optically active auxiliary agent since the separation of two enantiomers occurs during the course of crystallization. The resulting conglomerate is a mechanical mixture of enantiopure crystals, and the enantiomers can often be obtained from the conglomerate by sorting.[4]

The spontaneous resolution of metal supramolecules is still a relatively rare phenomenon, since the factors determining this process are not yet fully understood. Therefore, the spontaneous resolution has only been observed occasionally in the case of metal supramolecules including dinuclear double[5] and trinuclear triple helicates,[6] helical coordination polymers,[7] as well as hydrogen-bonded helical chains[8] and sheets, respectively.[9] In some of these examples, however it was expected that the *noncovalent intermolecular interactions* (coordination and hydrogen bonding,[9a] C−H···π and π···π stacking,[5,7d] Ag···Ag argentophilic interaction[7h]) controlled the homochiral aggregation of the metal complexes

* To whom correspondence should be addressed. Fax: 36 1 438 1143. Tel.: 36 1 438 1100. E-mail: deak@chemres.hu (A.D.), palg@chemres.hu (G.P.).

(1) (a) Feringa, B. L.; van Delden, R. A. *Angew. Chem. Int. Ed.* **1999**, *38*, 3418. (b) Oda, R.; Huc, I.; Schmutz, M.; Candau, S. J.; MacKintosh, F. C *Nature* **1999**, *399*, 566. (c) Moulton, B.; Zaworotko, M. J. *Chem. Rev.* **2001**, *101*, 1629. (d) Albrecht, M. *Chem. Rev.* **2001**, *101*, 3457. (e) Reinhoudt, D. N.; Crego-Calama, M. *Science* **2002**, *295*, 2403. (f) Whitesides, G. M.; Grzybowski, B. *Science* **2002**, *295*, 2418. (g) Yi, L.; Yang, X.; Lu, T.; Cheng, P. *Cryst. Growth Des.* **2005**, *5*, 1215. (h) Lehn, J.-M.; Rigault, A.; Siegel, J.; Harrowfield, J.; Chevrier, B.; Moras, D. *Proc. Natl. Acad. Sci. USA* **1987**, *84*, 2565. (i) Perez-Garcia, L.; Amabilino, D. B. *Chem. Soc. Rev.* **2002**, *31*, 342. (j) Meistermann, I.; Moreno, V.; Prieto, M. J.; Moldrheim, E.; Sletten, E.; Khalid, S.; Rodger, P. M.; Peberdy, J.C.; Isaac, C. J.; Rodger, A.; Hannon, M. J. *Proc. Natl. Acad. Sci. USA* **2002**, *99*, 5069. (k) Albrecht, M.; Dehn, S.; Raabe, G.; Fröhlich, R *Chem. Commun.* **2005**, 5690. (l) Qin, Z.; Jennings, M. C.; Puddephatt, R. P. *Chem.—Eur. J.* **2002**, *8*, 735. (m) Hasegawa, T.; Furusho, Y.; Katagiri, H.; Yashima, E. *Angew. Chem. Int. Ed.* **2007**, *46*, 5885.

(2) (a) von Zelewsky, A.; Mamula, O. *J. Chem. Soc., Dalton Trans.* **2000**, 219. (b) Knof, U.; von Zelewsky, A. *Angew. Chem. Int. Ed.* **1999**, *38*, 302. (c) Bark, T.; Düggeli, M.; Stoeckli-Evans, H.; von Zelewsky, A. *Angew. Chem. Int. Ed.* **2001**, *40*, 2848. (d) Wheaton, C. A.; Puddephatt, R. J. *Angew. Chem. Int. Ed.* **2007**, *46*, 4461.

(3) Katsuki, I.; Matsumoto, N.; Kojima, M. *Inorg. Chem.* **2000**, *39*, 3350.

(4) Flack, H. D. *Helv. Chim. Acta* **2003**, *86*, 905.

(5) Sun, Q.; Bai, Y.; He, G.; Duan, C.; Lin, Z.; Meng, Q. *Chem. Commun.* **2006**, 2777.

(6) Krämer, R.; Lehn, J.-M.; De Cian, A.; Fischer, J. *Angew. Chem., Int. Ed. Engl.* **1993**, *32*, 703.

10.1021/ic702059v CCC: $40.75
Published on Web 02/21/2008

and thus the spontaneous resolution of them upon crystallization. It is known that in the process of crystallization these noncovalent interactions also play a key role since they hold together the assembly of molecules, which underlie nucleation, and the structure of the resultant crystal.[10] Owing to the reversibility of noncovalent intermolecular interactions, the different supramolecular assemblies are often in equilibrium when their thermodynamic stabilities are comparable. This equilibrium ratio between different supramolecular assemblies largely depends on conditions (concentration, temperature, etc.)[11,12] and medium (solvent, template).[13,14] A solvent, therefore, can control the stability of the supramolecular assemblies, by acting as a template that selectively binds to and stabilizes one particular assembly. Moreover, there are cases where no obvious templating effects of the solvent have been noted.[13f] The link between *solvent-mediated kinetic processes of molecular assembly* in the liquid phase and ultimate crystal packing, however, is also not yet fully understood.[10]

As a continuance of our research work on gold(I) complexes of xanthene-based diphosphine ligand, 9,9-dimethyl-4,5-bis(diphenylphosphino)-xanthene (xantphos), we focused our interest on spontaneous resolution of gold(I) diphosphines.[15] We reported the first example of crystallization-induced spontaneous resolution of a binuclear gold(I) metallacycle, $[(AuNO_3)_2(xantphos)]$.[15] In this case, the nitrate anions played an important role in the homochiral C−H···O linking of the molecules into a 2D array, whereas short Au···π interactions have also been observed in the crystal.[15] We also synthesized the $[Au_2(xantphos)_2](NO_3)_2$ molecule in which two strands of xantphos are folded relative to each other and held together by two Au(I) ions.[15] As a result, the $[Au_2(xantphos)_2]^{2+}$ cation is in a figure-eight conformation, where the 16-membered ring contains one short 2.858(1) Å Au···Au linkage.[15] It is of interest to note that the figure-eight motif is chiral since it could have a left or right disposition of the intercrossing helices.[16] The $[Au_2(xantphos)_2](NO_3)_2$ complex crystallized in centrosymmetric space group *C*2/*c*, thus both right- and left-handed molecules were present in the crystal.[15] As we mentioned, spontaneous resolution more likely occurs when strong, selective, and directional hydrogen bonds are able to extend the neighboring chiral molecules into multidimensional arrays. A successful approach for preparing metallosupramolecules that interact with anions through hydrogen bonding (are hydrogen bonded with anions) can be realized by adding hydrogen bond donor function(s) to organic ligand.[17] The family of diphosphine ligands based on xanthene-type backbones is well developed since they are effective catalyst especially in regioselective hydroformylation reactions.[18] We selected the 4,6-bis(diphenylphosphino) phenoxazine (nixantphos) as a ligand that owing to its NH function can be useful in the construction of hydrogen-bonded gold(I) supramolecular assemblies. We assembled the $[Au_2(nixantphos)_2](NO_3)_2$ molecule from gold cations, nitrate anions, and achiral nixantphos ligands, and the complex contains a 16-membered $[Au_2(nixantphos)_2]^{2+}$ cationic ring in a chiral figure-eight conformation. Here we report the solvent-assisted spontaneous resolution of the $[Au_2(nixantphos)_2](NO_3)_2$ complex, where the chirality of the $[Au_2(nixantphos)_2]^{2+}$ building units by chirally discriminative interactions is extended into homochiral assembly. We also show that the homochiral versus heterochiral aggregation of the $[Au_2(nixantphos)_2](NO_3)_2$ supramolecules can be tuned by changing the solvent. To the best of our knowledge, this represents the first example of crystallization induced spontaneous resolution of a binuclear metallacycle showing figure-eight conformation.

Experimental Section

Materials and General Methods. All chemicals and solvents used for the syntheses were of reagent grade. The solvents for

(7) (a) Jiang, L.; Feng, X.-L.; Su, C.-Y.; Chen, X.-M.; Lu, T.-B. *Inorg. Chem.* **2007**, *46*, 2637. (b) Biradha, K.; Seward, C.; Zaworotko, M. J. *Angew. Chem. Int. Ed.* **1999**, *38*, 492. (c) Tabellion, F. M.; Seidel, S. R.; Arif, A. M.; Stang, P. J. *Angew. Chem. Int. Ed.* **2001**, *40*, 1529. (d) Siemeling, U.; Scheppelmann, I.; Neumann, B.; Stammler, A.; Stammler, H.-G.; Frelek, J. *Chem. Commun.* **2003**, 2236. (e) Chen, C.-Y.; Cheng, P.-Y.; Wu, H.-H.; Lee, H. M. *Inorg. Chem.* **2007**, *46*, 5691. (f) Ezuhara, T.; Endo, K.; Aoyama, Y. *J. Am. Chem. Soc.* **1999**, *121*, 3279. (g) Batten, S. R.; Hoskins, B. F.; Robson, R. *Angew. Chem., Int. Ed. Engl.* **1997**, *36*, 636. (h) Chen, X.-D.; Du, M.; Mak, T. C. W. *Chem Commun.* **2005**, 4417. (i) Catalano, V. J.; Malwitz, M. A.; Etogo, A. O. *Inorg. Chem.* **2004**, *43*, 5714.

(8) Khatua, S.; Stoeckli-Evans, H.; Harada, T.; Kuroda, R.; Bhattacharjee, M. *Inorg. Chem.* **2006**, *45*, 9619.

(9) (a) Li, M.; Sun, Q.; Bai, Y.; Duan, C.; Zhang, B.; Meng, Q. *Dalton Trans.* **2006**, 2572. (b) Sunatsuki, Y.; Ikuta, Y.; Matsumoto, N.; Ohta, H.; Kojima, M.; Iijima, S.; Hayami, S.; Maeda, Y.; Kaizaki, S.; Dahan, F.; Tuchagues, J.-P. *Angew. Chem. Int. Ed.* **2003**, *42*, 1614. (c) Yamada, M.; Ooidemizu, M.; Ikuta, Y.; Osa, S.; Matsumoto, N.; Iijima, S.; Kojima, M.; Dahan, F.; Tuchagues, J.-P. *Inorg. Chem.* **2003**, *42*, 8406.

(10) Davey, R. J.; Allen, K.; Blagden, N.; Cross, W. I.; Lieberman, H. F.; Quayle, M. J.; Righini, S.; Seton, L.; Tiddy, G. J. T. *CrystEngComm* **2002**, *4*, 257.

(11) (a) Fromm, K. M.; Saugé Doimeadios, J. L.; Robin, A. Y *Chem. Commun.* **2005**, 4548. (b) Kraus, T.; Budèšínsky, M.; Cvačk, J.; Sauvage, J.-P *Angew. Chem., Int. Ed.* **2006**, *45*, 258. (c) Baxter, P. N. W.; Khoury, R. G.; Lehn, J.-M.; Baum, G.; Fenske, D. *Chem.—Eur. J.* **2000**, *6*, 4140.

(12) Park, S. J.; Shin, D. M.; Sakamoto, S.; Yamaguchi, K.; Chung, Y. K.; Lah, M. S.; Hong, J.-I. *Chem.—Eur. J.* **2005**, *11*, 235.

(13) (a) Burchell, T. J.; Puddephatt, R. J. *Inorg. Chem.* **2005**, *44*, 3718. (b) Lam, R. T. S.; Belenguer, A.; Roberts, S. L.; Naumann, C.; Jarrosson, T.; Otto, S.; Sanders, J. K. M. *Science* **2005**, *308*, 667. (c) Djordjevic, B.; Schuster, O.; Schmidbaur, H. *Inorg. Chem.* **2005**, *44*, 673. (d) Huang, X.-C.; Zhang, J.-P.; Chen, X.-M. *J. Am. Chem. Soc.* **2004**, *126*, 13218. (e) Thuéry, P.; Villiers, C.; Jaud, J.; Ephritikhine, M.; Masci, B. *J. Am. Chem. Soc.* **2004**, *126*, 6838. (f) Mamula, O.; Lama, M.; Stoeckli-Evans, H.; Shova, S. *Angew. Chem. Int. Ed.* **2006**, *45*, 4940.

(14) (a) Suzuki, K.; Kawano, M.; Fujita, M. *Angew. Chem. Int. Ed.* **2007**, *46*, 2819. (b) Schweiger, M.; Seidel, S. R.; Arif, A. M.; Stang, P. J. *Inorg. Chem.* **2002**, *41*, 2556. (c) Uehara, K.; Kasai, K.; Mizuno, N. *Inorg. Chem.* **2007**, *46*, 2563. (d) Fujita, M.; Ibukuro, F.; Hagihara, H.; Ogura, K. *Nature* **1994**, *367*, 720. (e) Pirondini, L.; Stendardo, A. G.; Geremia, S.; Campagnolo, M.; Samori, P.; Rabe, J. P.; Fokkens, R.; Dalcanale, E. *Angew. Chem. Int. Ed.* **2003**, *42*, 1384.

(15) Deák, A.; Megyes, T.; Tárkányi, G.; Király, P.; Biczók, L.; Pálinkás, G.; Stang, P. J. *J. Am. Chem. Soc.* **2006**, *128*, 12668.

(16) (a) Karle, I. L.; Ranganathan, D.; Haridas, V. *J. Am. Chem. Soc.* **1996**, *118*, 10916. (b) Werner, A.; Michels, M.; Zander, L.; Lex, J.; Vogel, E. *Angew. Chem. Int. Ed.* **1999**, *38*, 3650.

(17) Hay, B. P.; Dixon, D. A.; Bryan, J. C.; Moyer, B. A. *J. Am. Chem. Soc.* **2002**, *124*, 182.

(18) (a) van der Veen, L. A.; Keeven, P. H.; Schoemaker, G. C.; Reek, J. N. H.; Kamer, P. C. J.; Leeuwen, P. W. N. M.; Lutz, M.; Spek, A. L. *Organometallics* **2000**, *19*, 872. (b) Bronger, R. P. J.; Kamer, P. C. J.; Leeuwen, P. W. N. M. *Organometallics* **2003**, *22*, 5358. (c) Ricken, S.; Osinski, P. O.; Eilbracht, P.; Haag, R. *J. Mol. Catal. A.* **2006**, *257*, 78.

Table 1. Crystal Data and Structure Refinement Parameters for Complexes **1** and **2**, Respectively

complex	1	2
empirical formula	$C_{72}H_{54}N_2O_2P_4Au_2$, 2 (NO_3) 3(CH_4O) (H_2O)	$C_{72}H_{54}N_2O_2P_4Au_2$, 2 (NO_3) 4(C_2H_3N)
formula mass	1735.16	1785.22
crystal size [mm]	0.15 × 0.29 × 0.30	0.18 × 0.21 × 0.35
color	orange	orange
crystal system	orthorhombic	monoclinic
space group	$P2_12_12_1$	$C2/c$
temp. (K)	103	103
θ range for data collection (°)	$3.1 \le \theta \le 25$	$3.1 \le \theta \le 25$
a [Å]	14.747(2)	21.985(5)
b [Å]	18.000(2)	15.655(3)
c [Å]	25.977(3)	22.109(4)
β [deg]	90	108.665(8)
V [Å^3]	6895.5(14)	7209 (3)
Z	4	4
d_{calc} [Mg/m^3]	1.671	1.645
μ [mm^{-1}]	4.409	4.218
$F(000)$	3440	3536
index ranges	$-16 \le h \le 17$	$-26 \le h \le 26$
	$-21 \le k \le 21$	$-18 \le k \le 18$
	$-30 \le l \le 30$	$-26 \le l \le 26$
no. of collected reflns.	83193	55823
no. of indep. reflns./R_{int}	12066/0.096	6358/0.130
no. of obsd. reflns. $I > 2\sigma(I)$	11143	5402
no. of parameters	871	463
GOOF	1.028	1.14
$R1$ (obsd. data)	0.0403	0.0555
$wR2$ (all data)	0.0904	0.1531
Flack parameter	−0.007(6)	-
largest diff. peak/ hole (e Å^{-3})	1.71/-1.03	1.38/-0.93

Scheme 1

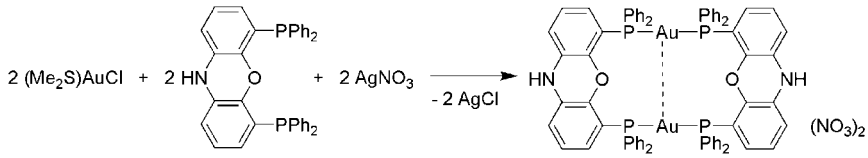

synthesis were used without further purification. All reactions were carried out at room temperature.

Synthesis of $[Au_2(nixantphos)_2](NO_3)_2$. A suspension of $(Me_2S)AuCl$ (0.2 g, 0.679 mmol) in 10 mL dichloromethane was treated with a suspension of nixantphos (0.3742 g, 0.679 mmol) in 10 mL dichloromethane and with $AgNO_3$ (0.1154 g, 0.679 mmol). The mixture was stirred for 6 h, shielded from light. The suspension was filtered off, washed with dichloromethane and diethyl ether. The precipitate was dissolved in methanol, filtered through Celite to remove the AgCl content, and then, the solvent was evaporated to yield a yellow product. Yield: 0.36 g (65.4%). Diffraction quality single crystals of $[Au_2(nixantphos)_2](NO_3)_2 \cdot 3MeOH \cdot H_2O$ (**1**) were obtained by slow diffusion of *n*-hexane into a CH_3OH solution of $[Au_2(nixantphos)_2](NO_3)_2$; mp > 300 °C. ^{1}H NMR (399.9 MHz, CD_2Cl_2, 25 °C): δ 5.50–5.61 (m, 2H), 6.64–6.76 (m, 4H), 6.81–7.58 (m, br, 18H), 7.60–7.71 (m, 2H), 9.89 (s, 1H); ^{1}H NMR (599.9 MHz, CD_2Cl_2, −80 °C): 5.51 (dd, $^3J_{HH}$ = 8.6 Hz, $^3J_{PH}$ = 8.6 Hz, 1H), 5.14 (dd, $^3J_{HH}$ = 8.8 Hz, $^3J_{PH}$ = 8.8 Hz, 1H), 6.50 (tr, $^3J_{HH}$ = 7.4 Hz, 2H), 6.63 (tr, $^3J_{HH}$ = 7.3 Hz, 1H), 6.67 (tr, $^3J_{HH}$ = 7.6 Hz, 1H), 6.79 (m, 1H), 6.91–7.01 (m, 3H), 7.01–7.09 (m, 3H), 7.09–7.22 (br, m 1H), 7.25 (br, 1H), 7.29 (tr, $^3J_{HH}$ = 7.4 Hz, 1H), 7.32–7.42 (m, 5H), 7.45 (tr, $^3J_{HH}$ = 7.1 Hz, 1H), 7.54 (tr, $^3J_{HH}$ = 7.1 Hz, 1H), 7.70 (tr, $^3J_{HH}$ = 7.1 Hz, 1H), 7.79 (tr, $^3J_{HH}$ = 7.4 Hz, 1H), 7.90–7.97 (m, 1H), 9.85 (br. 1H); ^{31}P NMR (161.9 MHz, CD_2Cl_2, 25 °C): δ 32.2; ^{31}P NMR (161.9 MHz, CD_2Cl_2, −80 °C): δ 33.1 (P_A), 32.1 (P_B).

Crystals of $[Au_2(nixantphos)_2](NO_3)_2 \cdot 4MeCN$ (**2**) were obtained by slow diffusion of *n*-hexane into a CH_3CN solution; mp > 300 °C.

Single Crystal X-ray Diffraction. Crystal data and data collection and refinement details for **1** and **2** are listed in Table 1. Crystals of **1** and **2** were mounted in Paratone-N oil within a conventional cryo-loop, and intensity data were collected on a Rigaku R-AXIS RAPID image plate diffractometer (λ(Mo Kα radiation) = 0.71070 Å), fitted with an X-stream low temperature attachment at 103 K. Several scans in the φ and ω direction were made to increase the number of redundant reflections, which were averaged over the refinement cycles. The structures were solved by direct method (SIR92)[19] and refined by full-matrix least-squares (SHELXL-97).[20] All calculations were carried out using the *WinGX* package of crystallographic programs.[21] All nonhydrogen atoms were refined anisotropically in F^2 mode. Hydrogen atomic positions were generated from assumed geometries. The riding model was applied for the hydrogen atoms. A value of −0.007(6) was obtained for the Flack parameter of **1**, which indicated that the correct configuration had been obtained.

NMR Experiments. NMR experiments were carried out on a Varian Inova (400 MHz for ^{1}H) and Varian NMR System (600 MHz for ^{1}H) spectrometers using switchable broadband X{^{1}H} probes (X = ^{31}P). Samples were placed into 5 mm NMR tubes. ^{1}H chemical shifts are referenced to the residual solvent signal (CD_2Cl_2: 5.32 ppm). ^{31}P shifts are given relative to the external reference 85% H_3PO_4. Deuterated (99.98 atom%) solvents were purchased from Merck GmBH, Germany. Phosphorus spectra were recorded by recording 10240 scans with 5 s recycle delays and continuous

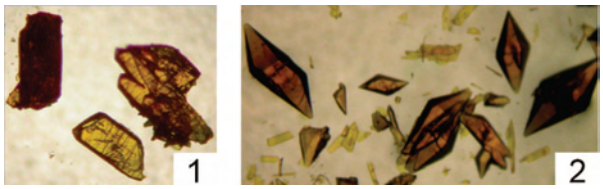

Figure 1. Microscopic images of the crystals of **1** and **2**, respectively.

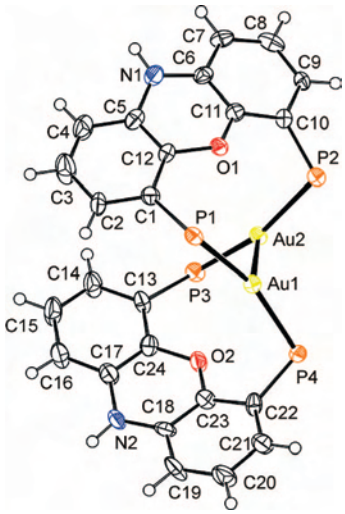

Figure 2. Ortep view of the cationic skeleton of **1** (the phenyl groups are omitted for clarity), illustrating the 16-membered ring containing gold(I) showing the figure-eight conformation. Ellipsoids are shown at the 50% probability level.

WALTZ proton decoupling. Spectra were processed and simulated by the standard spectrometer software package: VnmrJ 2.1B.

Results and Discussion

The reaction of $(Me_2S)AuCl$ with nixantphos and $AgNO_3$ in a molar ratio of 1:1:1 in dichloromethane yields the $[Au_2(nixantphos)_2](NO_3)_2$ complex (Scheme 1).

Crystallization of the chiral or the other racemic crystal is simply determined by the solvent used to crystallization, methanol or acetonitrile, respectively. The $[Au_2(nixantphos)_2]$-$(NO_3)_2 \cdot 3MeOH \cdot H_2O$ (**1**) obtained from hydrous methanol crystallized in the noncentrosymmetric, orthorhombic space group $P2_12_12_1$, while the $[Au_2(nixantphos)_2](NO_3)_2 \cdot 4MeCN$ (**2**) complex was obtained from acetonitrile and crystallized in the centrosymmetric, monoclinic space group $C2/c$. The crystals of **1** and **2** have apparently differentiable habits (morphologies, Figure 1).

The X-ray structural data of both **1** and **2** indicate that they consists of $[Au_2(nixantphos)_2]^{2+}$ cations in which two strands of nixantphos are folded relative to each other and held together by two Au(I) ions (Figures 2 and 3). Selected bond lengths and angles are given in Table 2. Each gold atom in **1** is coordinated by two phosphorus atoms in a nearly linear geometry, exhibiting P(1)−Au(1)−P(4) and P(2)−Au(2)−P(3) angles of 160.4(1) and 160.9(1)°, respectively. The coordination geometry at the gold atoms in **2** is

(19) Altomare, A.; Cascarano, G.; Giacovazzo, C.; Guagliardi, A.; Burla, M. C.; Polidori, G.; Camalli, M. *J. Appl. Cryst.* **1994**, *27*, 435.
(20) Sheldrick, G. M. *SHELXL97-Program for the Refinement of Crystal Structures*; University of Göttingen: Germany, 1997.
(21) Farrugia, L. J *J. Appl. Cryst.* **1999**, *32*, 837.

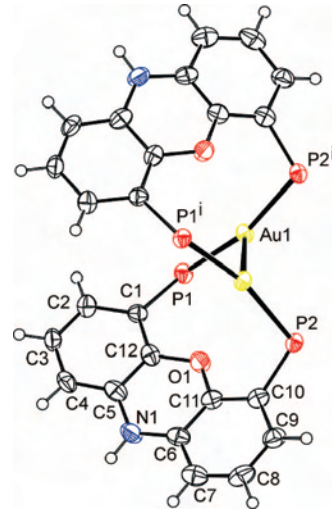

Figure 3. Ortep view of the cationic skeleton of **2** (the phenyl groups are omitted for clarity), illustrating the 16-membered ring showing the figure-eight conformation [equivalent atoms generated by $i = (2 - x, y, {}^3/_2 - z)$]. Ellipsoids are shown at the 50% probability level.

Table 2. Selected Bond Lengths (Å) and Angles (deg) for **1** and **2**, Respectively[a]

1		2	
Au(1)···Au(2)	2.862(1)	Au(1)···Au(1)^i	2.856(1)
Au(1)−P(1)	2.314(2)	Au(1)−P(1)	2.332(3)
Au(1)−P(4)	2.325(2)	Au(1)−P(2)^i	2.347(2)
Au(2)−P(2)	2.326(2)		
Au(2)−P(3)	2.315(2)		
P(1)−Au(1)−P(4)	160.4(1)	P(1)−Au(1)−P(2)^i	162.6(1)
P(2)−Au(2)−P(3)	160.9(1)		

[a] Equivalent atoms are generated by $i = (2 - x, y, {}^3/_2 - z)$.

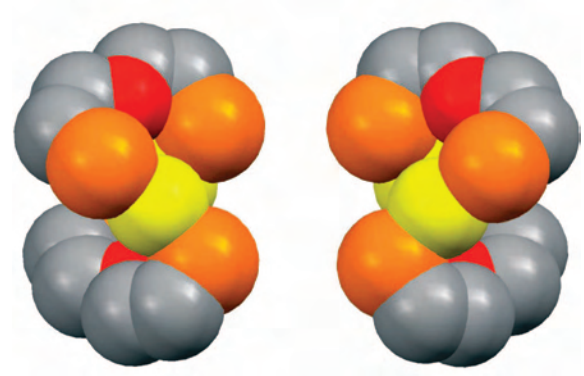

Figure 4. Two enantiomers of the 16-membered ring containing gold(I) showing a figure-eight conformation.

also nearly linear, with P(1)−Au(1)−P(2)^i angle of 162.6(1)°. The Au−P distances, which lie in the range 2.314(2)−2.326(2) Å in **1**(Table 2) are similar to those found in complex **2**. In complex **1**, the ligand backbones are folded and tilted by 84.1(1)° [P(1)−Au(1)−Au(2)−P(2)] and 81.7(1)° [P(4)−Au(1)−Au(2)−P(3)] with respect to the Au···Au axis, and the two nixantphos ligands bridge the Au(I) ions to form a short aurophilic attraction of 2.862(1) Å. This backbone folding around the Au···Au axis in **2** is 84.8(1)° [P(1)−Au(1)−Au(1)^i−P(2)], and the Au···Au distance is 2.856(1) Å. With this short aurophilic Au···Au attraction taken into account, the molecules of **1** as well as **2** exist in a figure-eight conformation, as shown in Figure 4. The Au···Au bond distance in complexes with aurophilic

interaction ranges from 2.70 to 3.30 Å,[22] and often governs the organization of gold compounds into supramolecular associations.[23] The strengths of this aurophilic interactions have been determined experimentally to be well beyond that of conventional van der Waals interactions and to be typically in the range of 7−12 kcal·mol^{-1}, which is comparable to that of hydrogen bonding.[24]

As determined by single crystal X-ray diffraction, the crystal of **1** contains only one of the two enantiomers, either right- or left-handed in contrast to **2**, which contains both $[Au_2(nixantphos)_2](NO_3)_2$ enantiomers. Refinement of the Flack parameter led to a value of ~0, which confirms the enantiomeric purity of the crystal of **1**.

As shown in Figure 5, the molecules of **1** are linked throughout N−H···O and C−H···O interactions into a 2D helix. This is achieved in such a way that one of the nitrate anions with its O(3) and O(4) atoms is involved as an acceptor in the N−H···O hydrogen bonding, and establishes the connection between neighboring $[Au_2(nixantphos)_2]^{2+}$ cations. These N−H···O and additional C−H···O interactions link the $[Au_2(nixantphos)_2]^{2+}$ cations and nitrate anions into *homochiral helices* along the 2_1 axis (Table 3). The second nitrate anion with its O(7) oxygen atom is involved as an acceptor in the C−H···O hydrogen bonding with a methanol molecule, which is also C−H···O linked with another methanol. The O(9) oxygen atom of this methanol acting as donor and acceptor establishes the O−H···O hydrogen bonding with water molecule (Figure 6, Table 3). As observed in the spontaneous resolution of the $[(AuNO_3)_2$-(xantphos)] complex,[15] the role of the nitrate anion played in the N−H···O and C−H···O linking of the molecules is chirally discriminative and required that complex **1** exhibits the same absolute configuration.

In contrast to **1**, where only one of the two enantiomers, either right- or left-handed is present, the crystal of **2** contains both right- and left-handed molecules. In crystal of **2**, the N−H···O hydrogen bond formed between the NH function of the $[Au_2(nixantphos)_2]^{2+}$ cation and O(3) and O(4) atoms of the NO_3^- anion is bifurcated, since the NH group straddles these oxygen atoms of the nitrate. The remaining third oxygen of the anion interacts with the MeCN solvent molecule forming a short C−H···O contact (Table 3). As illustrated in Figure 7, both right- and left-handed enantiomers of $[Au_2(nixantphos)_2]^{2+}$ cation are N−H···O bonded to NO_3^- anions, which in their turn are C−H···O bonded to MeCN solvent molecules. Therefore, the solvent excludes

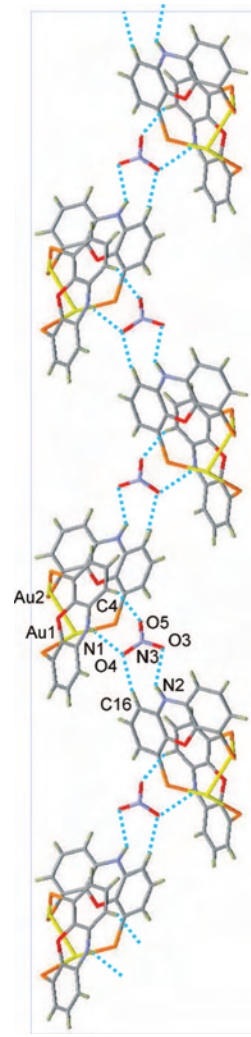

Figure 5. View illustrating the N−H···O and C−H···O bonded homochiral helices of $[Au_2(nixantphos)_2]^{2+}$ cations and NO_3^- anions in the crystal structure of **1**.

the intermolecular hydrogen-bonding between the enantiomers. The main difference between **1** and **2** arises from different hydrogen bonding behavior of the nitrate anions. In crystal of **1**, one type of nitrate anions is involved in N−H···O and C−H···O hydrogen-bonded homochiral helix formation of $[Au_2(nixantphos)_2]^{2+}$ cations, whereas the second type of nitrate anions is part of the C−H···O hydrogen-bonding aggregation with solvent molecules. In contrast to this, in the crystal of **2**, the same nitrate anion is linked to both $[Au_2(nixantphos)_2]^{2+}$ cation and solvent molecule by N−H···O and C−H···O contacts, respectively. Recently, a 16-membered twisted $C_8NP_4Au_3$ ring with a Möbius topology has been reported, and in this case, the right- and left-handed metallamacrocycles are linked into dimers by C−H···O interactions.[25]

The dissolved complexes **1** and **2** were characterized by ^{1}H and ^{31}P NMR spectroscopy. It is noted that low solubility (<1 mM) of the samples was a major drawback of the NMR analyses. Nevertheless, the NMR properties of the $[Au_2(nixantphos)_2]^{2+}$ cation are found to be rather similar

(22) (a) Schmidbaur, H.; Graf, W.; Müller, G. *Angew. Chem., Int. Ed. Engl.* **1988**, *27*, 417. (b) Schmidbaur, H. *Gold Bull.* **2000**, *33*, 3.

(23) (a) Schmidbaur, H. *Nature* **2001**, *413*, 31. (b) Brandys, M.-C.; Jennings, M. C.; Puddephatt, R. J. *J. Chem. Soc., Dalton Trans.* **2000**, 4601. (c) Brandys, M.-C.; Jennings, M. C.; Puddephatt, R. J. *J. Chem. Soc., Dalton Trans.* **2000**, 4601. (d) Irwin, M. J.; Vittal, J. J.; Yap, G. P. A.; Puddephatt, R. J. *J. Am. Chem. Soc.* **1996**, *118*, 13101. (e) Wheaton, C. A.; Eisler, D. J.; Jennings, M. C.; Puddephatt, R. J. *J. Am. Chem. Soc.* **2006**, *128*, 15370. (f) Burchell, T. J.; Eisler, D. J.; Jennings, M. C.; Puddephatt, R. P. *Chem Commun.* **2003**, 2228. (g) Chen, J.; Mohamed, A. A.; Abdou, H. E.; Krause Bauer, J. A., Jr.; Bruce, A. E.; Bruce, M. R. M. *Chem. Commun.* **2005**, 1575. (h) Deák, A.; Tunyogi, T.; Tárkányi, G.; Király, P.; Pálinkás, G. *CrystEngComm* **2007**, *9*, 640. (i) Lee, Y.-A.; Eisenberg, R. *J. Am. Chem. Soc.* **2003**, *125*, 7778.

(24) Hollatz, C.; Schier, A.; Schmidbaur, H *Inorg. Chim. Acta* **2000**, *300–302*, 191.

(25) Kui, S. C. F.; Huang, J.-S.; Wai-Yin Sun, R.; Zhu, N.; Che, C.-M *Angew. Chem., Int. Ed.* **2006**, *45*, 4663.

Table 3. Selected Interatomic Distances (Å) and Angles (deg) for Complexes **1** and **2**

complex	D−H···A	symmetry code (*i*)	H···A (Å)	D···A (Å)	D−H···A (deg)
1	N(1)−H(1N)···O(4)^i	$1 + x, y, z$	2.39	3.07(1)	135
	N(2)−H(2N)···O(3)^i	$1 - x, \frac{1}{2} + y, \frac{3}{2} - z$	2.26	2.88(1)	127
	C(4)−H(4)···O(5)^i	$1 + x, y, z$	2.30	3.11(2)	143
	C(16)−H(16)···O(4)^i	$1 - x, \frac{1}{2} + y, \frac{3}{2} - z$	2.47	3.34(2)	152
	C(4A)−H(4A)···O(3)^i	$\frac{3}{2} - x, 2 - y, \frac{1}{2} + z$	2.60	3.48(1)	155
	O(9)−H(9A)···O(12)		2.34	2.94(2)	129
	O(12)−H(12A)···O(9)		2.33	2.94(2)	129
	C(26)−H(26A)···O(9)		1.83	2.79(2)	164
	C(26)−H(26B)···O(7)		2.15	2.75(2)	118
2	N(1)−H(1)···O(3)^i	$\frac{3}{2} - x, -\frac{1}{2} + y, \frac{3}{2} - z$	2.59	3.14(2)	121
	N(1)−H(1)···O(4)^i	$\frac{3}{2} - x, -\frac{1}{2} + y, \frac{3}{2} - z$	1.98	2.85(2)	168
	C(15)−H(15A)···O(2)^i	$2 - x, 1 - y, 2 - z$	2.30	2.92(3)	121

to the $[Au_2(xantphos)_2]^{2+}$ cation characterized previously.[26] First, some resonances in the proton spectrum are broadened at room temperature owing to the moderately fast chemical exchange related to the interconversion of the enantiomeric skeletons of the 16-membered macrocycle in solution (see Supporting Information Figure S1). This conformational process is achieved by the simultaneous changes in the P1−Au1−Au2−P3 and P2−Au2−Au1−P4 torsions, which interconverts the P1/P2 and P4/P3 phosphorus atoms (Figure 8). Although solution NMR spectroscopy (achiral) is unable to distinguish the two enantiomers, the racemization process is detected via the chemical exchange between P1 and P2 as well as between P4 and P3. A similar dynamic process has also been described for a trinuclear double stranded gold(I) helicate.[27]

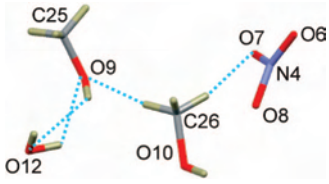

Figure 6. O−H···O and C−H···O hydrogen-bonded aggregate of one nitrate anion, two methanols, and a water molecule in the crystal structure of **1**.

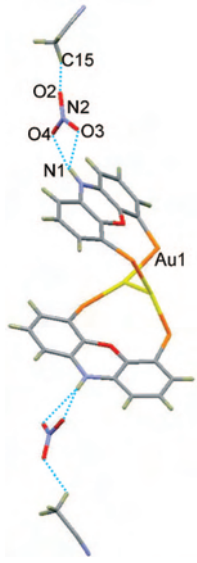

Figure 7. View illustrating the N−H···O bonded $[Au_2(nixantphos)_2]^{2+}$ cation and NO_3^- anions, where the anions are also C−H···O bonded with acetonitrile molecules in the crystal structure of **2**.

This conformational motion becomes slow on the chemical shift time scale when the system is cooled down in dichloromethane, allowing a more practical spectral characterization of the system (see Supporting Information Figure S2). The low temperature ^{1}H NMR spectra of **1** and **2** appeared to be identical within experimental error. Second, the ^{31}P NMR spectrum which is an averaged singlet at 25 °C ($\delta = 32.2$ ppm) becomes an AA′BB′ ^{31}P-multiplet at −80 °C (Figure S3). The appearance of this particular spin-system is the characteristics of the short aurophilic contact $[Au_2(nixantphos)_2]^{2+}$ within the figure-eight conformation of the macrocyclic skeleton having C_2 symmetry in solution.

We have performed spin-system analysis (Figure 9) on the experimental low temperature ^{31}P spectrum and assessed the four ^{31}P−^{31}P scalar coupling constants ($^2J(P_A,P_B) = 321.0$ Hz, $^3J(P_A,P_{B'}) = 7.8$ Hz, $^3J(P_B,P_{B'}) = 3.3$ Hz, $^3J(P_A,P_{A'}) =$

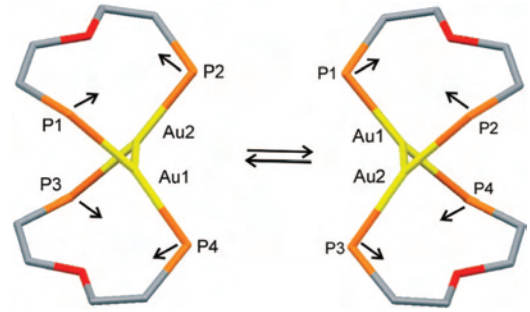

Figure 8. Conformational exchange process in solution which interconverts the arbitrarily labeled P1/P2 and P4/P3 phosphorus atoms of the 16-membered macrocycle.

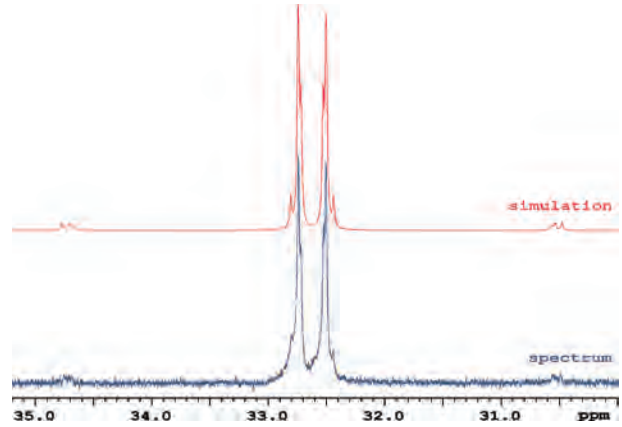

Figure 9. ^{31}P NMR (161.9 MHz, CD_2Cl_2, 1 mM) spectrum of **1** measured at −80 °C (bottom) and the spin-system simulation for the AA′BB′ system (top).

0.6 ± 0.4 Hz) and the two chemical shift values ($\delta(P_A)$ = 33.1 ppm, $\delta(P_B)$ = 32.1 ppm). The large two-bond $^2J_{AB}$ coupling, which is in good agreement with the roughly linear geometry of the P−Au−P moiety, dominates the appearance of the spin-system. With no electron lone-pairs on the phosphorus atoms the three-bond $^{31}P-^{31}P$ *J*-couplings are transferred only via the Au···Au bond verifying the existence of this latter.

Conclusion

The crystals of both the homochiral hydrogen bonded helices (**1**) and heterochiral hydrogen bonded monomers (**2**) of the $[Au_2(nixantphos)_2](NO_3)_2$ enantiomers were successfully obtained by changing the nature of the surrounding solvent medium. It is conceivable that the triplex hydrogen bonding acceptor motif of trigonal planar nitrate is suitable for controlling the molecular alignment in well-defined supramolecular architectures, and the chirality of the crystal (homochiral versus heterochiral) can be tuned by subtle changes in solvent system. In conclusion, we have found that the triplex hydrogen bonding acceptor motif of nitrate anion could work as a new type of supramolecular connecting motif based on homochiral recognition. According to NMR experiments, the 16-membered macrocycle retains its helically distorted conformation at −80 °C in solution. At this temperature the aurophilic interaction has been proven via ^{31}P NMR spin-system analysis of the AA′BB′ ^{31}P-multiplet.

Acknowledgment. We gratefully acknowledge the financial support of this work by Hungarian Scientific Research Funds (OTKA) K68498 and GVOP-3.2.1.-2004-04-0210/3.0 projects. The authors are indebted to Prof. Peter Stang for his continuous interest and support.

Supporting Information Available: Crystallographic files in CIF format for compounds **1** and **2**, and Figures S1−S3 showing the room temperature ^1H NMR spectrum of **1**, low temperature ^1H NMR spectra of **1** and **2**, and room and low temperature ^{31}P NMR spectra of **1**. This material is available free of charge via the Internet at http://pubs.acs.org.

IC702059V

(26) Tárkányi, G.; Király, P.; Pálinkás, G.; Deák, A. *Magn. Reson. Chem.* **2007**, *45*, 917.
(27) Schuh, W.; Kopacka, H.; Wurst, K.; Peringer, P. *Chem. Commun.* **2001**, 2186.